Pergamon

Solid State Communications, Vol. 107, No. 5, pp. 227–231, 1998

0038-1098/98 $19.00+.00

PII: S0038-1098(98)00191-4

ELECTRONIC STRUCTURES OF CHIRAL CARBON TOROIDS

Ming-Fa Lin,* Rong-Bin Chen and Feng-Lin Shyu

Department of Physics, National Cheng Kung University, Tainan, Taiwan 70101, The Republic of China

(*Received* 22 *January* 1998; *accepted* 7 *April* 1998 *by S. Ushioda*)

The π-electronic states of chiral carbon toroids are calculated from the tight-binding model. The electronic structures, the energy gap, the energy spacing and the degeneracy of discrete states, are studied. They are mainly determined by the geometric structures (height, chiral angle and radius) the curvature effect and the magnetic flux (ϕ). Carbon toroids have four (three) types of energy gaps, while the curvature effect is important (negligible). The relations between energy gaps and geometric structures are complex (simple) in the presence (absence) of the curvature effect. The ϕ-dependent electronic structures exhibit the periodic Aharonov-Bohm oscillations. The magnetic flux could also effectively affect the state degeneracy of zigzag carbon toroids. © 1998 Elsevier Science Ltd. All rights reserved

Keywords: D. electronic band structure, A. fullerenes, A. nanostructures.

Carbon atoms could form diamond, graphite, carbon nanotubes (CNs; [1]), carbon toroids (CTs; [2]), C_{60}-related fullerenes [3] and carbon onions [4]. These systems have various geometric structures, which include three, two, one and zero dimensions. The electronic structures strongly depend on the geometric structures and so do other physical properties. They could exhibit many interesting physical properties. For example, diamond is the hardest material. Carbon toroids were recently reported by Liu *et al.* [2]. The toroid radius is $R \sim 1500$–2500 Å and the toroid height or width is $2r \sim 10$ Å. The former is much larger than the latter; that is, a CT is very thin. As a result of the cylindrical symmetry, a thin CT in the presence of magnetic flux (ϕ) would exhibit the periodical Aharonov–Bohm (AB) oscillations. Here we mainly study the electronic structures of chiral CTs. The dependence on the toroid height, the chiral angle (θ), the toroid radius, the curvature effect and the magnetic flux is investigated. Density of states (DOS) is also included in the calculations.

In general, CTs could be constructed from CNs by: (1) bending a long nanotube (length ~ 1 μm) and directly connecting the two ends together (this work [2]), (2) connecting small sliced parts of the nanotubes [5] and (3) connecting two sections of identical turnover bilayer nanotube ends at the equator of the resulting toroid [6]. Concerning CTs built from the last two methods, they are not discovered in experiments up to now. The ratio between the toroid radius and the toroid height, $R/2r$, is typically smaller than 10. To stabilize such toroids, there exist certain pentagons and heptagons instead of hexagons. Their geometric structures and thus electronic structures quite differ from those studied in this work [2].

The geometric and electronic structures of a thin CT are closely related to those of a cylindrical CN or a graphite sheet. A cylindrical CN could be regarded as a graphite sheet rolled from the origin to the vector $\mathbf{R}_x = m\mathbf{a}_1 + n\mathbf{a}_2$ [7, 8]. $\mathbf{a}_1$ and $\mathbf{a}_2$ are the primitive vectors of a graphite sheet. The radius and the chiral angle of a (m,n) CN are, respectively, $r = |\mathbf{R}_x|/2\pi = b\sqrt{3(m^2 + mn + n^2)}/2\pi$ and $\theta = \tan^{-1}[-\sqrt{3}n/(2m+n)]$. That the chiral angle is confined to $0° \le |\theta| \le 30°$ is sufficient [7]. $b = 1.42$ Å is the C–C bond length. Carbon atoms are arranged on a nanotube surface in a helical fashion except for zigzag ($\theta = 0°$ and $m = 0$) and armchair ($\theta = -30°$ and $m = n$) nanotubes. A CT is formed, while a cylindrical CN further bends along the tubular axis and the origin also coincides with the vector $\mathbf{R}_y = p\mathbf{a}_1 + q\mathbf{a}_2$. That is to say, a CT corresponds to a rolled-up graphite sheet which satisfies the transverse ($\|\mathbf{R}_x$) and the longitudinal ($\|\mathbf{R}_y$) periodical boundary conditions simultaneously. A carbon

* Corresponding author.

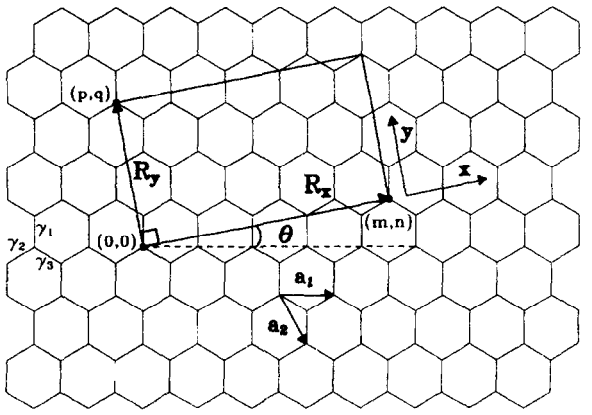

Fig. 1. A cylindrical carbon nanotube is regarded as a graphite sheet rolled from the origin to the vector $\mathbf{R}_x = m\mathbf{a}_1 + n\mathbf{a}_2$. $\mathbf{a}_1$ and $\mathbf{a}_2$ are the primitive vectors of a graphite sheet. The chiral angle, θ, is defined as the angle between the rolled direction (x-axis) and the zigzag direction ($\|\mathbf{a}_1$). A carbon toroid is formed, when a cylindrical nanotube further bends along the tubular axis and the origin coincides with the vector $\mathbf{R}_y = p\mathbf{a}_1 + q\mathbf{a}_2$.

toroid is uniquely characterized by the parameters (m, n, p, q). There are two kinds of achiral CTs, zigzag $(m, 0, p, -2p)$ and armchair $(m, m, p, -p)$ CTs. The former (latter) have the zigzag (armchair) and the armchair (zigzag) structures along the transverse and the longitudinal directions, respectively.

The π-electronic states of CTs come from carbon $2p_z$ orbitals. They are calculated with the nearest-neighbor tight-binding Hamiltonian like the one employed for a graphite sheet [9] or a CN [7], but here with the proper periodical boundary conditions along the transverse and the longitudinal directions. Due to the curvature along the transverse direction, the π-electron orbitals are generally not parallel to one another. When the curvature effect is taken into consideration [10], the resonance integrals, $(\gamma_1, \gamma_2, \gamma_3)$ (Fig. 1), along the different directions might differ slightly. The π-electron state energies of the (m, n, p, q) toroid in the presence of magnetic flux, obtained by diagonalizing the Hamiltonian, are

$$E(J, L, \phi) = \pm [x_1^2 + 4x_1x_2 \cos\alpha \cos 3\beta + 4x_2^2 \cos^2\alpha + 4x_1x_3 \sin\alpha \sin 3\beta + 4x_3^2 \sin^2\alpha]^{1/2}, \quad (1a)$$

where

$$x_1 = \gamma_1 = \gamma_0\left[1 - \frac{b^2 \sin^2\theta}{8r^2}\right], \quad (1b)$$

$$x_2 = \frac{\gamma_3 + \gamma_2}{2} = \gamma_0\left[1 - \frac{b^2(2\cos^2\theta + 1)}{32r^2}\right], \quad (1c)$$

$$x_3 = \frac{\gamma_3 - \gamma_2}{2} = \gamma_0\left[\frac{\sqrt{3}b^2 \sin 2\theta}{32r^2}\right], \quad (1d)$$

$$\alpha = \pi\left[\frac{J\cos\theta}{\sqrt{m^2 + mn + n^2}} - \frac{(L + \phi/\phi_0)\sin\theta}{\sqrt{p^2 + pq + q^2}}\right], \quad (1e)$$

$$\beta = \frac{\pi}{\sqrt{3}}\left[\frac{J\sin\theta}{\sqrt{m^2 + mn + n^2}} + \frac{(L + \phi/\phi_0)\cos\theta}{\sqrt{p^2 + pq + q^2}}\right]. \quad (1f)$$

γ_0 is the resonance integral without the curvature effect [7, 9]. $J = 1, 2, \ldots, N_u/2$ ($L = 1, 2, \ldots, N_v$) are the angular momenta along the transverse (longitudinal) direction. $N_u = 4\sqrt{(m^2 + mn + n^2)(p^2 + pq + q^2)}/3$ and N_v is the maximum common factor of (p, q). They could serve as the state index. + and − signs outside the square-root sign are, respectively, the antibonding states (π^* states) and the bonding states (π states). The former are symmetric to, about $E_F = 0$, the latter. Hence the Fermi level keeps there during variation of magnetic flux. The Zeeman splitting energy, $g\sigma\phi/m_eR^2\phi_0$ ($\phi_0 = hc/e$), is negligible except for large ϕ (e.g. $\phi \sim 100\phi_0$).

The electronic structures depend on the geometric structures (including height, radius and chiral angle), the curvature effect and the magnetic flux. A CT has many discrete states ($\sim 10^5$ states) and the energy spacing is small (~ 1 meV). It is similar to a macro-molecule. The energy gap, E_g, is the energy difference between the highest occupied states (HOS) and the lowest occupied states (LUS). The low energy electronic properties are related to energy gap.

The three types of energy gaps in the absence of curvature effect (i.e. $\gamma_1 = \gamma_2 = \gamma_3 = \gamma_0$) are simply reviewed [11, 12]. At $\phi = 0$, the energy gap of a (m, n, p, q) CT is $E_g = \gamma_0 b/r$ (type I) for $2m + n \neq 3i$ (i is an integer), $E_g = 0$ (type II) for $2m + n = 3i$ and $2p + q = 3i$ and $E_g = \gamma_0 b/R$ (type III) for others. A type I CT with $2m + n \neq 3i$ is insensitive to magnetic flux as well as curvature effect. However, other CTs could drastically change from type II into type III or *vice versa* as magnetic flux varies. $E_g(\phi)$ is a linearly periodical function, with a period ϕ_0. At $0 \leq \phi \leq \phi_0/2$, $E_g(\phi) = 3\gamma_0 b\phi/R\phi_0$ for $2m + n = 3i$ and $2p + q = 3i$ and $E_g(\phi) = 3\gamma_0 b|3\phi - \phi_0|/3R\phi_0$ for $2m + n = 3i$ and $2p + q \neq 3i$.

There are four types of energy gaps, inclusive of the curvature effect. The ϕ-dependent energy gap, type I expected, could be simplified expressed as

$$E_g(\phi) = 2\gamma_0\left[\left(\frac{3b^2\cos 3\theta}{32r^2}\right)^2 + \frac{9b^2(\phi - \phi_a)^2}{4R^2\phi_0^2}\right]^{1/2}. \quad (2)$$

ϕ_a is the magnetic flux corresponding to the minimum energy gap. It is dependent on height, chiral angle and radius. $\phi_a = 0$ for the zigzag $(m, 0, p, -2p)$ CTs, but the simple relations between ϕ_a and (r, θ, R) are absent for

others. If the first term inside the square-root sign is neglected, $E_g(\phi)$ in equation (2) is energy gap without curvature effect. Under such a condition, ϕ_a is, respectively, equal to 0 and $\phi_0/3$ for $2p+q=3i$ and $\neq 3i$.

At $\phi=0$, the four types of energy gaps include $E_g \simeq \gamma_0 b/r$, 0, $\gamma_0 b/R$ and $2\gamma_0[(3b^2\cos 3\theta/32r^2)^2+9b^2\phi_a^2/4R^2\phi_0^2]^{1/2}$ (type IV; $\theta \neq 30°$). Only the gapless type II CTs are metals and the others are semiconductors. The type I, II, III and IV CTs correspond to $2m+n\neq 3i$, $m=n$, $m=n$, and others, respectively. Only a little armchair $(m, m, p, -p)$ CTs are type II metals, e.g. $E_g \sim 10^{-6}\,\gamma_0$ for the (10, 10, 4849, −4849) CT (not shown). Most of armchair CTs belong to type III semiconductors, e.g. $E_g \sim 1.05\times 10^{-3}\,\gamma_0$ for the (27, 27, 5001, −5001) CT (the light solid curve in Fig. 2). For type IV CTs with $r<5$ Å, $E_g \sim 3\gamma_0 b^2\cos 3\theta/16r^2$ are independent of magnetic flux.

The magnetic flux could effectively alter the low energy electronic structures except for type I CTs. $E_g(\phi)$, as shown in Fig. 2, is periodical with period ϕ_0 and it is symmetric about $\phi_0/2$. When magnetic flux varies, the armchair $(m, m, p, -p)$ CTs could change from narrow-gap semiconductors (type III) into gapless metals (type II), or *vice versa*, e.g. the (27, 27, 5001, −5001) CT. As for type IV CTs magnetic flux does not thoroughly alter the characteristics of energy gaps, i.e. E_gs remain finite at any ϕ. However, E_g might be significantly affected by ϕ. Energy gaps of all chiral CTs are first reduced to the minimum values at ϕ_as and then increase during the variation of ϕ, e.g. $E_g(\phi)$ of the (30, 24, 4797, −5166) CT (the dashed-circled curve). Only energy gaps of the zigzag $(m, 0, p, -2p)$ are enhanced by ϕ, e.g. $E_g(\phi)$ of the (48, 0, 2887, −5774) CT (the heavy solid curve). They are given by $E_g = 2\gamma_0[(3b^2/32r^2)^2+9b^2\phi^2/4R^2\phi_0^2]^{1/2}$.

The effects of the geometric structures on the electronic structures deserve a closer investigation. For CTs with nearly the same height and radius (Fig. 2), the minimum ϕ-dependent energy gap, $E_{\min}$, would decrease from $3\gamma_0 b^2/16r^2$ to zero, when the chiral angle increases from 0° to 30°. It further illustrates that only the armchair carbon toroids could exhibit the metallic behavior. Moreover, $E_g(\phi)$ strongly depends on the toroid radius and the toroid height, as shown in Fig. 3. Also noticed that $E_{\min}$ is independent of the toroid radius. In general, the oscillational amplitude of $E_g(\phi)$ is larger for CTs with smaller radii and heights. Such kinds of CTs are suggested to be more suitable in verifying the periodical AB effect, e.g. the periodical persistent currents in CTs [11]. In short, carbon toroids exhibit four (three) types of energy gaps, when the curvature effect is important (negligible). The relations between energy gaps and geometric structures are complicated (simple) in the presence (absence) of the curvature effect. The characteristics of the low energy electronic structures would be reflected in certain physical properties, such as persistent currents. Experimental measurements could be used to verify whether the curvature effect is obvious.

Density of states is useful in further understanding the low energy electronic structures. It is defined as

$$D(w,\phi) = 2\sum_{J,L}\frac{\Gamma}{\pi[(E(J,L,\phi)-w]^2+\Gamma^2}. \qquad (3)$$

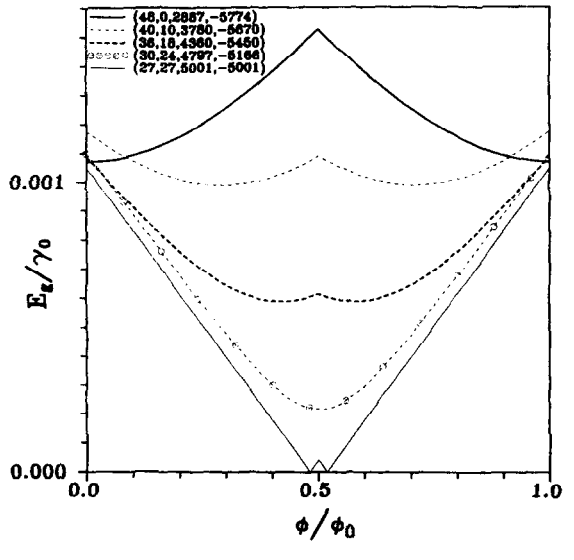

Fig. 2. The smallest energy difference (E_g) between the highest occupied state and the lowest unoccupied state is periodical in magnetic flux (ϕ). It is shown for various carbon toroids with nearly the same height and radius.

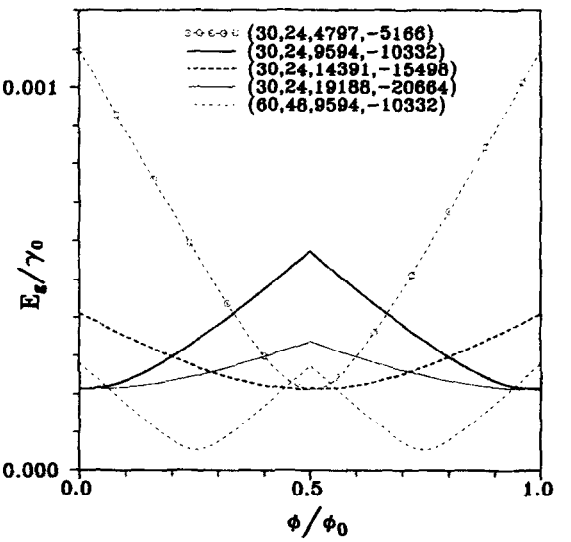

Fig. 3. Same plot as Fig. 2, but shown for carbon toroids with different radii and widths.

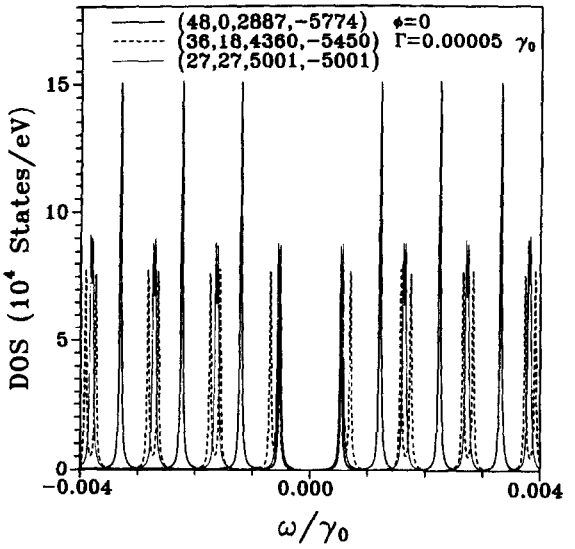

Fig. 4. Density of states (DOS) is shown for various carbon toroids at $\phi = 0$.

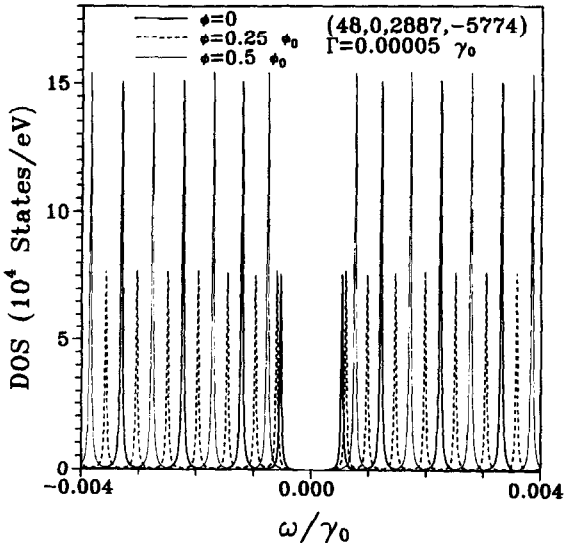

Fig. 5. Same plot as Fig. 4, but shown for the (48, 0, 2887, −5774) toroid at different ϕs.

The factor of 2 accounts for the two spins. Γ is the broadening parameter and $\Gamma = 5 \times 10^{-5}\,\gamma_0$ is used in the calculations. DOS at $\phi = 0$ is shown in Fig. 4. It is vanishing (prominent) at the neighborhood of $w = 0$ for semiconducting (metallic) CTs. DOS exhibits pronounced peaks at ws, where the discrete states exist. Their heights are related to the degeneracy of electronic states. The energy spacing relies on the chiral angle and the toroid radius, but the degeneracy only on the former. The electronic states of the zigzag CTs are fourfold degeneracy except that the states nearest to the Fermi level are double degeneracy, e.g. the (48, 0, 2887, −5774) CT. That $E(J,L) = E(N_u/2-J,L) = E(J,N_v-L) = E(N_u/2-J,N_v-L)$ [$E(J,L) = E(N_u/2-J,L)$ for HOS and LUS] is the main reason. Other CTs exhibit double degeneracy because of $E(J,L) = E(N_u/2-J,L)$. The state energies, as shown in Fig. 5, clearly vary with magnetic flux. The zigzag CTs also change from the fourfold degeneracy into the double degeneracy at $\phi \neq i\phi_0$ and $i\phi_0/2$. In addition, the electronic states of other CTs are double degeneracy at any ϕ. The state energies and the degeneracy of electronic states, which mainly depend on geometric structures and magnetic flux, could be identified by the electronic excitations [13].

In conclusion, we have calculated the π-electronic states of chiral carbon toroids. The state energies could be expressed as an analytic form. A carbon toroid has $\sim 10^5$ states, which is similar to a macromolecule. The electronic structures, the energy gap, the energy spacing and the degeneracy of discrete states, are investigated. In general, the dependence on the toroid height, the chiral angle, the toroid radius, the curvature effect [10] and the magnetic flux, is strong. Carbon toroids are predicted to have four (three) types of energy gaps, while the curvature effect is important (negligible). The relations between energy gaps and geometric structures are complicated (simple) in the presence (absence) of curvature effect. For example, the minimum ϕ-dependent energy gap would decrease from a finite value to zero as the chiral angle increases from 0° to 30°. The ϕ-dependent electronic structures exhibit the periodical AB oscillations. The magnetic flux could also effectively affect the state degeneracy of zigzag carbon toroids. The characteristics of the electronic structures would be directly reflected in other physical properties, such as magnetic [11] and optical properties [13]. Experimental measurements could be used to test the theoretical predictions. For example, they could verify whether the curvature effect on the low energy electronic structures is obvious.

Acknowledgement—This work was supported in part by the National Science Council of Taiwan, the Republic of China under the Grant No. NSC 87-2112-M-006-019.

REFERENCES

1. Ijima, S., *Nature*, **354,** 1991, 56.
2. Liu, J., Dai, H., Hafner, J.H., Colbert, D.T., Smalley, R.E., Tans, S.J. and Dekker, C., *Nature*, **385,** 1997, 780.
3. Kroto, H.W., Heath, J.R., O'Brien, S.C., Curl, R.F. and Smalley, R.E., *Nature*, **318,** 1985, 162.
4. Ugarte, U., *Nature*, **359,** 1992, 707.
5. Dunlap, B.I., *Phys. Rev.*, **B46,** 1992, 1933.
6. Itoh, S., Ihara, S. and Kitakami, J.I., *Phys. Rev.*, **B47,** 1993, 1703; **B47,** 1993, 12908; **B48,** 1993, 8323.

7. Saito, R., Fujita, M., Dresselhaus, G. and Dresselhaus, M.S., *Appl. Phys. Lett.*, **60,** 1992, 2204.
8. Lin, M.F. and Shung, K.W.-K., *Phys. Rev.*, **B52,** 1995, 8423.
9. Wallace, P.R., *Phys. Rev.*, **71,** 1947, 622.
10. Kane, C.L. and Mele, E.J., *Phys. Rev. Lett.*, **78,** 1997, 1932.
11. Lin, M.F. and Chuu, D.S., *Phys. Rev.*, **B57,** 1998, 6731.
12. Lin, M.F. and Chuu, D.S., *J. Phys. Soc. Jpn.*, **67,** 1998, 259.
13. Lin, M.F. (unpublished).